UNVEILING THE WAVE CONCEPT IN ELECTROMAGNETIC THEORY: APPLICATION TO THE TRANSVERSE WAVE APPROACH FOR MICROWAVE SYSTEMS ANALYSIS

Zeineb KLAI[1], Mohamed Ali HAMMAMI[2]

Numerical methods have established their efficacy in diverse domains, including electric machines, telecommunications, radar systems, and digital computing. Within this paradigm, the Wave Concept emerges as a pivotal tool for accelerating these methods. By transforming integral formulations of the electromagnetic (EM) field into algebraic problems within the framework of Hilbert space methods, the Wave Concept facilitates enhanced computational efficiency.

This paper delves into the development of the Wave Concept and its application within the Transverse Wave Approach, shedding light on its utility in addressing EM field challenges. The Transverse Wave Approach is explored as a method to convert integral formulations into algebraic problems, offering a novel perspective on problem-solving within the electromagnetic domain. To gauge its computational effectiveness, a comprehensive evaluation is conducted in the specific context of microwave systems. The outcomes of this investigation contribute to a deeper understanding of the Transverse Wave Approach's potential impact on advancing numerical methods in electromagnetics.

Keywords: Wave Concept, Numerical EM methods, Computational Effort, Microwave Systems

1. Introduction

Numerical methods play an indispensable role in electromagnetic (EM) simulations, offering a comprehensive toolkit for tackling complex challenges across various domains. These methods, encompassing finite element methods [1], finite difference methods [2], boundary element methods [3], the Discontinuous Galerkin method [4-6], and the Method of Moments (MoM) [7], enable the detailed modeling and analysis of EM phenomena. By converting complex EM problems into manageable mathematical formulations, they facilitate in-depth exploration of wave propagation, radiation, and material interactions.

[1] PhD., Faculty of Sciences of Sfax, University of Sfax, Tunisia ; Faculty of Computing and Information Technology, Northern Border University –Kingdom of Saudi Arabia, e-mail: Zeineb.klai@nbu.edu.sa

[2] Prof., Faculty of Sciences of Sfax, University of Sfax, Tunisia, e-mail: mohamedali.hammami@fss.rnu.tn

The efficiency of these numerical methods is critical, as it directly affects their feasibility and scalability. This efficiency hinges on the computational effort required to solve the vast systems of equations that arise from discretizing EM governing equations. The criteria for assessing method efficiency include accuracy, convergence speed, and computational time, with ongoing advancements in computational resources and algorithms playing a key role in enhancing these aspects.

Numerical EM methods are employed in a wide range of applications, from electric machines [8] and telecommunications [9] to radar systems [10] and microwave devices [11]. They equip engineers and researchers with the means to design and optimize devices, forecast performance, and tackle EM field-related challenges, serving as a foundational toolkit for understanding and leveraging electromagnetic phenomena. The continuous enhancement of computational efficiency not only expands their application scope but also makes substantial contributions across technologically essential sectors.

This paper introduces the wave concept technique as a novel contribution to numerical EM methods, aiming to streamline the analysis process. By transforming integral formulations or differential equations into algebraic ones, the wave concept technique significantly reduces computational complexities. This innovative approach, which we justify and detail in the subsequent sections, particularly emphasizes the transverse wave approach for implementing EM solutions. Our work seeks to push the boundaries of numerical EM methods, offering a powerful tool for rapid simulations and enhanced problem-solving capabilities in electromagnetic studies.

The organization of this paper is as follows: Section 2 presents the theoretical background and the mathematical foundations of the wave concept technique. Section 3 discusses the implementation of this technique within the framework of the transverse wave approach, while Section 4 is dedicated to validating and discussing the outcomes of various simulations. Finally, Section 5 concludes our work, summarizing the key findings and contribution.

2. Wave Concept: Theory

2.1. Adopted Mathematical Formalism

In this investigation, Ω represents a bounded, open, and connected set in $\mathbb{R}^2$, serving as the designated measure space (definition domain) for the exploration of electromagnetic (EM) fields within the realm of radiofrequency (RF) integrated circuits applications. The functions introduced in subsequent sections conform to the L2-norm, allowing for the manipulation of magnitudes possessing finite energy. The space $L^2(\Omega)$ signifies the standard Lebesgue square-integrable or square-summable C-valued functions.

By introducing an inner product structure on L^2 with respect to a measure μ, we establish this vectorial space as the unique Hilbert space within the broader class of L^P spaces ($1 \leq p \leq \infty$) [12]. Using Dirac notation, the functions within this Hilbert space adhere to the following expressions:

$$\forall \varphi, \psi \in L^2(\Omega) \quad \langle \varphi | \psi \rangle = \iint_\Omega \varphi^* \psi d\mu \tag{1}$$

$$\forall \varphi \in L^2(\Omega) \quad \|\varphi\|_2 = \sqrt{\langle \varphi | \varphi \rangle} \tag{2}$$

Here, the symbol * denotes the complex conjugate. Additional properties of Hilbert space are elaborated in Appendix A.

2.2. Maxwell's Equations and the Propagation Wave Equation

Analyzing electromagnetic fields in distinct spatial regions is paramount for understanding the propagation and interaction of EM waves. These regions can be categorized based on their geometric uniformity: uniform regions possess consistent cross-sectional areas, whereas non-uniform regions exhibit varied geometrical features. This distinction is crucial in the study of electromagnetic fields within cylindrical waveguides, which present uniform cross sections, and more complex structures like non-cylindrical waveguides, each demanding a tailored analytical approach. The electromagnetic field behavior in these settings is often modeled as a superposition of standard wave functions, facilitating a bridge between theoretical predictions and practical engineering applications, particularly at ultrahigh frequencies.

Central to this analysis are Maxwell's equations, which describe the dynamics of electric (E) and magnetic (H) fields, serving as the cornerstone for the theoretical underpinnings of electromagnetic signal propagation [13]. The empirical validation of these equations by Hertz in 1886 ushered in the era of practical radio wave applications, highlighting their integral role in modern communications. These equations can be represented in both differential and integral forms, accommodating analyses in the time domain and emphasizing the behavior of time-varying electromagnetic fields.

In the realm of electromagnetic theory, the application of sinusoidal or time-harmonic sources is predominant, owing to their relevance in frequency-specific applications. The employment of phasor solutions in this context, analogous to the concept of rotating phasors in circuit theory, significantly simplifies the analysis of electromagnetic fields, particularly for single or narrow-band frequencies. This simplification is essential for elucidating the phasor domain representations of electric and magnetic fields, as detailed in Appendix B-1, offering a foundational understanding of EM wave behavior across various mediums.

Maxwell's equations delineate key vectors such as electric field intensity (E) and magnetic field intensity (H), further expanded upon by constitutive relations that incorporate electric and magnetic polarizations, permeability (μ), and permittivity (ϵ), tailored for linear, non-dispersive media. These relationships are encapsulated in equations (3) to (6), providing a mathematical framework for the interaction between electric and magnetic fields within specified materials.

$$\mathcal{D} = \varepsilon_0 \mathcal{E} + \mathcal{P}_e = \varepsilon_0 \left(1 + \chi_e\right) \mathcal{E} = \varepsilon_0 \varepsilon_r \mathcal{E} = \varepsilon \mathcal{E} \tag{3}$$

$$\mathcal{B} = \mu_0 \mathcal{H} + \mathcal{P}_m = \mu_0 \left(1 + \chi_m\right) \mathcal{H} = \mu_0 \mu_r \mathcal{H} = \mu \mathcal{H} \tag{4}$$

$$\varepsilon_r = \varepsilon' - j\varepsilon'' = \varepsilon' \left(1 - j \tan \delta_e\right),\ \tan \delta_e = \frac{\omega \varepsilon'' + \sigma_e}{\omega \varepsilon'} \tag{5}$$

$$\mu_r = \mu' - j\mu'' = \mu' \left(1 - j \tan \delta_m\right),\ \tan \delta_m = \frac{\omega \mu'' + \sigma_m}{\omega \mu'} \tag{6}$$

In our analysis, particularly in the context of vacuum or hollow waveguides, the inclusion of a fictitious magnetic charge in Table 2 serves as a theoretical tool to symmetrize Maxwell's equations [22][23]. This strategic incorporation enhances analytical clarity while acknowledging that both the electric charge density and the magnetic charge density are zero, in accordance with established principles [22][23]. It's important to emphasize that this utilization does not imply the physical existence of magnetic monopoles. Rather, it aligns with well-established methodologies [24][25], facilitating a deeper understanding of electromagnetic wave propagation in structurally complex environments such as waveguides.

Our recognition of the theoretical nature of magnetic monopoles is consistent with broader scientific consensus [24][25], underscoring the utility of employing non-physical constructs to elucidate complex electromagnetic phenomena.

The synergy between electric and magnetic fields gives rise to the generation of electromagnetic waves, a phenomenon that surpasses the constraints of lumped-element models. Central to the propagation of these waves is the complex propagation constant (γ), which encompasses both the attenuation and phase progression of electromagnetic waves within a medium. Equation (7), outlined in Appendix B-2, provides a comprehensive expression for γ, accommodating a wide range of material properties.

$$\nabla^2 F + \gamma^2 F = 0 \tag{7}$$

where F refers to E or H

$$\frac{\partial^2 F_X}{\partial z^2} - \gamma^2 F_X = 0 \tag{8}$$

$$F_X\left(z, j\omega\right) = \underbrace{F^+\left(j\omega\right) e^{-j\gamma z}}_{Positive-going\ wave} + \underbrace{F^-\left(j\omega\right) e^{j\gamma z}}_{Negative-going\ wave} \tag{9}$$

$$V(z) = \underbrace{V_+ e^{-\gamma z}}_{Incident\ wave} + \underbrace{V_- e^{\gamma z}}_{Reflected\ wave} \tag{10}$$

$$I(z) = Z_c^{-1}\left(V_+ e^{-\gamma z} - V_- e^{\gamma z}\right) \tag{11}$$

The wave equation (8) and its solution (9) demonstrate the positive and negative propagation of waves, providing insights into incident and reflected waves. The wave equation's analogy with distributed circuits is expressed in equations (10) and (11), incorporating characteristic impedance (*Z*c). The figure presented below depicts a case of a uniform transmission line.

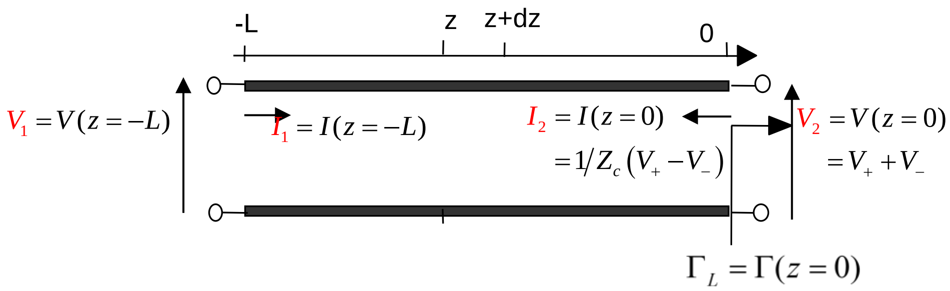

Fig. 1. Example of uniform transmission line

The Poynting vector delineates the density of power flux or instantaneous power. In the context of time-harmonic fields, equations (12) and (13) introduce the phasor Poynting vector and average power density, respectively. The direction of power flow, as determined by the right-hand rule, is consistently perpendicular to both the electric and magnetic fields. Equation (14) quantifies the total average power traversing a surface (S).

$$P = E \times H^* \tag{12}$$

$$P_{AV} = \frac{1}{2} Re(E \times H^*) \tag{13}$$

$$P_{T_{AV}} = \frac{1}{2} Re \iint_S (E \times H) \cdot dS \tag{14}$$

2.3. Wave Concept

The significance of the Wave Concept becomes apparent through the exploration of waveguide principles. Waveguides, diverse in forms like conducting or dielectric cylinders, twisted wire pairs, coaxial conductors, or single wires, play a crucial role in directing energy along a specific path without radiating into the surroundings. Hollow waveguides [14], particularly vital in microwave technology for low attenuation and high-power applications, serve as fundamental elements in microwave circuits.

The behavior of propagating waves in waveguides is intricately tied to the concept of modes, solutions to Maxwell's equations that adhere to necessary boundary conditions. Each mode within a waveguide exhibits a unique pattern for electric and magnetic fields, contributing to the overall characteristics of the guided energy. Waveguides typically feature a countable set of modes, each with a cutoff frequency dictating its propagation range. Hollow conducting cylinders, including rectangular and circular waveguides, constitute a significant waveguide class. Propagation of modes in such waveguides is contingent on the wavelength being smaller than the largest cross-sectional dimension. Even configurations with non-separable geometries or bends can be effectively analyzed using numerical electromagnetic methods.

The classification of waveguide modes encompasses TEM (Transverse Electromagnetic), TE (Transverse Electric), TM (Transverse Magnetic), and Hybrid modes, each characterized by specific field patterns. The expressions for field intensities are deconstructed based on translational invariance along the waveguide as follows:

$$E = E_T(x, y)e^{\pm\gamma z} \tag{15}$$

$$H = H_T(x, y)e^{\pm\gamma z} \tag{16}$$

where

$$\gamma = \underbrace{\alpha}_{\substack{\text{Evanescent}\\ \text{modes}}} + \underbrace{j\beta}_{\substack{\text{Propagating}\\ \text{modes}}} \tag{17}$$

Modes within waveguides can be further categorized into propagating and evanescent modes, distinguished by the nature of their propagating coefficients. Subdividing an electromagnetic structure into substructures allows for complete sets of modal field solutions, forming a basis for expanding field solutions and ensuring alignment with boundary conditions.

The utilization of modal basis functions within a function space is a key aspect of numerical electromagnetic methods, notably the Method of Moments (MoM)[7]. This approach provides precise solutions, enabling expansions in TEmn and TMmn modes and contributing to a comprehensive understanding of waveguide behavior.

Let k serve as a concise notation representing the double index *mn* for TE*mn* and TM*mn* modes. Summation over k implies a sum over all TE*mn* and TM*mn* modes. The total transverse field is expressed as a superposition of transverse modes:

$$E_T(z) = \sum_k \left(V_k^{(+)} e^{-\gamma_k z} + V_k^{(-)} e^{\gamma_k z} \right) \cdot e_k(u,v) \tag{18}$$

$$H_T(z) = \sum_k \frac{1}{Z_{W,k}} \left(V_k^{(+)} e^{-\gamma_k z} - V_k^{(-)} e^{\gamma_k z} \right) \cdot h_k(u,v) \tag{19}$$

The electric and magnetic structure vectors are orthogonal at any point and the structure forms $e_k(u,v)$ and $h_k(u,v)$ fulfill:

$$e_k(u,v) = -\left(dz \wedge h_k(u,v)\right)^* \tag{20}$$

$$h_k(u,v) = \left(dz \wedge e_k(u,v)\right)^* \tag{21}$$

Here (u,v,z) represents a general cylindrical coordinate system, where z is a linear coordinate, and u,v are orthogonal curvilinear coordinates transverse to z.

The structures forms $e_k(u,v)$ and $h_k(u,v)$constitute an orthogonal basis:

$$\langle e_k | h_l \rangle_S = -\langle h_k | e_l \rangle_S = \delta_{kl} \tag{22}$$

where δ_{kl} denotes the Kronecker symbol.

With the equation (21), we can represent the fields by Hilbert space vectors as:

$$|E_T(z)\rangle = \sum_k \left(V_k^{(+)} e^{-\gamma_k z} + V_k^{(-)} e^{\gamma_k z} \right) \cdot |e_k\rangle \tag{23}$$

$$|H_T(z)\rangle = \sum_k \frac{1}{Z_{W,k}} \left(V_k^{(+)} e^{-\gamma_k z} - V_k^{(-)} e^{\gamma_k z} \right) \cdot |h_k\rangle \tag{24}$$

where the $|e_k\rangle$and $|h_k\rangle$ constitute a bi-orthogonal set of basis vectors. The electric and magnetic field expressions can be determined by calculating them from their respective Hilbert space vectors through:

$$E_T(z) = \sum_k e_k(u,v) \langle h_k | E_T \rangle \tag{25}$$

$$H_T(z) = \sum_k \frac{1}{Z_{W,k}} h_k(u,v) \langle e_k | H_T \rangle \tag{26}$$

We define the wave impedance operator by:

$$\hat{\boldsymbol{Z}}_{\boldsymbol{W}} = \sum_{n=1}^{\infty} Z_{W,k} \left(|h_n\rangle\langle e_n| - |e_n\rangle\langle h_n| \right) \tag{27}$$

Its inverse termed wave admittance operator is given by:

$$\hat{\boldsymbol{Y}}_{\boldsymbol{W}} = \sum_{n=1}^{\infty} Y_{W,k} \left(|h_n\rangle\langle e_n| - |e_n\rangle\langle h_n| \right) = \sum_{n=1}^{\infty} Z_{W,k}^{-1} \left(|h_n\rangle\langle e_n| - |e_n\rangle\langle h_n| \right) \tag{28}$$

With this we introduce the wave amplitude vectors $|\vec{A}\rangle$ and $|\vec{B}\rangle$ as

$$\left|\vec{A}\right\rangle = \frac{1}{2}\left[|E_T\rangle + \boldsymbol{Z_W}|H_T\rangle\right] \tag{29}$$

$$\left|\vec{B}\right\rangle = \frac{1}{2}\left[|E_T\rangle - \boldsymbol{Z_W}|H_T\rangle\right] \tag{30}$$

We compute the transverse electric and magnetic fields form the wave amplitudes via

$$|E_T\rangle = \left|\vec{A}\right\rangle + \left|\vec{B}\right\rangle \tag{31}$$

$$|H_T\rangle = \boldsymbol{Z_W}^{-1}\left(\left|\vec{A}\right\rangle - \left|\vec{B}\right\rangle\right) \tag{32}$$

We introduce the operator $\widehat{\boldsymbol{\Gamma}}(z)$ and its inverse as

$$\widehat{\boldsymbol{\Gamma}}(z) = \sum_{n=1}^{\infty} e^{-\gamma_k z}\left(|h_n\rangle\langle e_n| - |e_n\rangle\langle h_n|\right) \tag{33}$$

$$\widehat{\boldsymbol{\Gamma}}^{-1}(z) = \sum_{n=1}^{\infty} e^{\gamma_k z}\left(|h_n\rangle\langle e_n| - |e_n\rangle\langle h_n|\right) \tag{34}$$

Consequently, and referring to (28), the equation (33) can be expressed as:

$$\widehat{\boldsymbol{\Gamma}}(z) = \left(\widehat{\boldsymbol{I}} + Z_W\widehat{\boldsymbol{Y}}_{\boldsymbol{W}}(z)\right)^{-1}\left(\widehat{\boldsymbol{I}} - Z_W\widehat{\boldsymbol{Y}}_{\boldsymbol{W}}(z)\right) \tag{35}$$

where $\widehat{\boldsymbol{I}}$ is the identity operator.

3. Application of Wave Concept in Transverse wave approach

Drawing from the wave concept introduced in the preceding section, solving electromagnetic (EM) problems becomes feasible without resorting to intensive computations required for resolving integral formulations or differential equations. Within this framework, the wave concept is founded on the linear combination of the transverse electric field (E_T) and the transverse magnetic field (H_T). This combination facilitates the derivation of incident and reflected at the discontinuity interface. The combinations between both incident $\vec{A}_r$ and reflected $\vec{B}_r$ waves can be expressed in matrix form by:

$$\begin{vmatrix}\vec{A}_r\\ \vec{B}_r\end{vmatrix} = \widehat{\boldsymbol{M}}\begin{vmatrix}\vec{E}_T^r\\ \vec{H}^r{}_T \times \vec{n}_r\end{vmatrix} = \widehat{\boldsymbol{M}}\begin{vmatrix}\vec{E}_T^r\\ \vec{J}_T^r\end{vmatrix} \tag{36}$$

$\widehat{\boldsymbol{M}}$ ensures the transition between integral EM field and algebraic EM wave:

$$\widehat{\boldsymbol{M}} = \frac{1}{2}\begin{vmatrix}Z_{0r}^{-\frac{1}{2}} & Z_{0r}^{\frac{1}{2}}\\ Z_{0r}^{-\frac{1}{2}} & -Z_{0r}^{\frac{1}{2}}\end{vmatrix} \tag{37}$$

Here Z_{0r} denotes the real wave impedance from region *r* defined by:

$$Z_{0r} = \sqrt{\frac{\mu_0}{\varepsilon_0 \varepsilon_{r_r}}} \qquad (38)$$

Also, Equation (39) defines the average power density (P_{AV}) in a region (r) as the difference between the power of the incident wave ($\left|\vec{A}_r\right|^2$) and the power of the reflected wave ($\left|\vec{B}_r\right|^2$).

$$P_{AV} = \frac{1}{2} Re\left(\vec{E}_T^r \times \vec{J}_T^{r*}\right) = \left|\vec{A}_r\right|^2 - \left|\vec{B}_r\right|^2 \qquad (39)$$

This mathematical representation, rooted in the conservation of energy, suggests that the power generated within the region is balanced by subtracting the power dissipated and the rate of stored energy increase. While the physical interpretation of this equation poses challenges, it can be understood as the incident wave contributing to energy generation in the region, while the reflected wave encapsulates the combined effects of dissipated power and the rate of stored energy increase within that region.

Leveraging the principles of the wave concept, the Transverse Wave Approach (TWA) [15-20] is introduced into numerical electromagnetic methods. In contrast to traditional approaches that rely solely on electric fields or current density, TWA operates through their linear combination. This methodology yields highly precise simulation results while minimizing computational complexity, eliminating the necessity for matrix inversion. Importantly, TWA guarantees convergence irrespective of the structure's interfaces and imposes no constraints on component shapes. It proficiently handles bounded operators, avoiding the inversion of integral operators. By iteratively addressing integral relations in the spectral domain and continuity conditions in the spatial domain, TWA adeptly distinguishes the topological characteristics of circuits from their embedding environment.

The TWA iterative process hinges on interconnected equations repeated until a solution is reached. The spatial domain initially formulates incident waves to meet electromagnetic field boundary conditions based on the excitation source. In contrast, reflected waves are expressed in the modal domain, considering electromagnetic wave properties in homogeneous media.

Assuming an excited structure, like a bilateral source polarized in the x-direction, generating waves on both sides of the discontinuity surface Ω, the iterative process unfolds. Each iteration sees incident waves (A_1, A_2) diffracted by the obstacle, creating new reflected waves (B_1, B_2). These reflected waves contribute to subsequent incident waves in successive iterations until system convergence.

The interaction between incident (A) and reflected (B) waves is represented by the equations:

$$\begin{cases} A = \widehat{\boldsymbol{\Gamma}} B \\ B = \widehat{\boldsymbol{S}} A + B_0 \end{cases} \tag{40}$$

Here, $\widehat{\boldsymbol{\Gamma}}$ is the reflection operator connecting incident and reflected waves in the modal domain, while $\widehat{\boldsymbol{S}}$ is the diffraction operator linking incident and reflected waves in the spatial domain.

B_0 represents the global excitation wave on the source.

The time efficiency comparison between the direct method, involving the resolution of integral and differential equations, and the numerical method, specifically the Transverse Wave Approach (TWA) based on the wave concept, is unequivocal. The computational effort for the direct method exhibits a complexity of $O(n^3)$ [7], indicating a cubic relationship with the problem size. In contrast, the TWA falls into the linearithmic class $\left(O(nlog\, n)\right)$, showcasing a remarkable reduction in the number of operations required for computation.

4. Results & Discussion

To validate the Transverse Wave Approach (TWA) utilizing the wave concept, a comprehensive analysis was conducted on a printed rectangular spiral antenna with significant applications, particularly in the field of biomedicine [21]. The simulation employed specific modeling and geometric parameters detailed in Table 1. The simulations were conducted utilizing our proprietary EM tool developed in C++, which is based on the Transverse Wave Approach (TWA) derived from the wave concept.

Table 1

Modeling and geometric parameters of the rectangular spiral antenna

Geometric Parameters	Description	Modeling Parameters	Description
Initial Length	0.19487mm	Resonance Frequency	60Ghz
Initial Height	0.12991mm	Type of polarization	Bilateral in x-direction
Number of Arms	2	Number of iterations	$N_{iter} = 100$
Number of turns	1.53		
Conductor	Copper	Waveband	$F_{min} = 30GHz$
Conductivity	5.96e+4 (S/mm)		$F_{max} = 70GHz$
Thickness	0.03556 mm		$Step_{F_{rq}} = 0.5GHz$

The critical parameter, impedance (Zin) or admittance (Yin), as perceived by the excitation source, was meticulously calculated for each iteration based on electromagnetic quantities. This parameter plays a pivotal role in determining the convergence of the system.

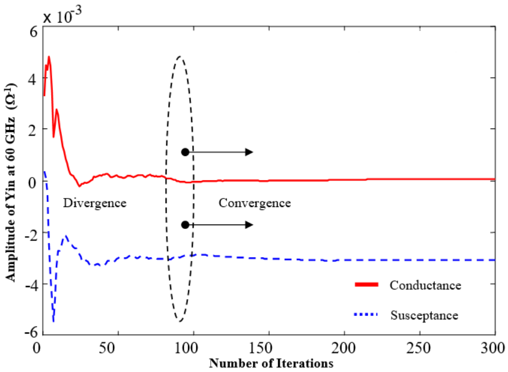

Fig. 2. Convergence Analysis of Admittance (Yin) Observed by the Excitation Source Over Iterations

Fig.2 serves as a compelling visual confirmation of the Transverse Wave Approach's (TWA) convergence, showcasing remarkable stability achieved in fewer than 100 iterations. This convergence assessment is conducted at a representative frequency of 60 GHz, emphasizing the efficiency of the TWA in swiftly reaching a solution.

Delving into Fig.3-(a), a more nuanced analysis of the admittance (Yin) is presented. Specifically, the real part, representing conductance, manifests peaks at resonance frequencies, signifying maximum values. Simultaneously, the imaginary part, indicative of susceptance, adeptly identifies sign changes at these resonant frequencies. These observed behaviors align seamlessly with electromagnetic theory, offering a robust and theoretically consistent representation.

The distinctive peaks in the conductance reveal the antenna's heightened responsiveness at resonance frequencies, emphasizing its optimal performance during these specific conditions. Meanwhile, the sign changes in susceptance underscore dynamic shifts in the antenna's reactive components, providing valuable insights into the intricate interplay of electric fields.

This comprehensive frequency-dependent profile of admittance, encompassing both conductance and susceptance, enhances our understanding of the antenna's response across varying frequencies. Such insights are instrumental in tailoring antenna designs to specific frequency requirements, ensuring optimal performance in resonance conditions. Overall, the detailed analysis presented in Fig.3-(a) not only validates the TWA's convergence but also offers a deeper understanding of the antenna's behavior through its admittance characteristics.

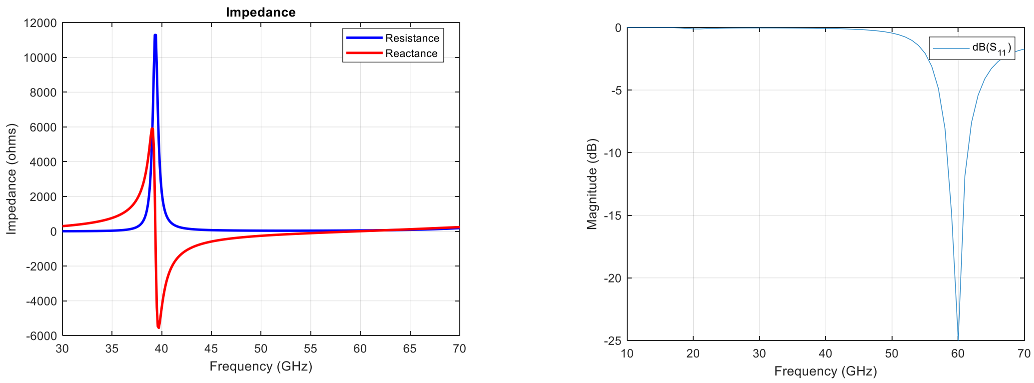

Fig. 3. Frequency-Dependent Evolution of (a) Reflection Coefficient S11(dB) and (b) Impedance (Conductance and Susceptance)

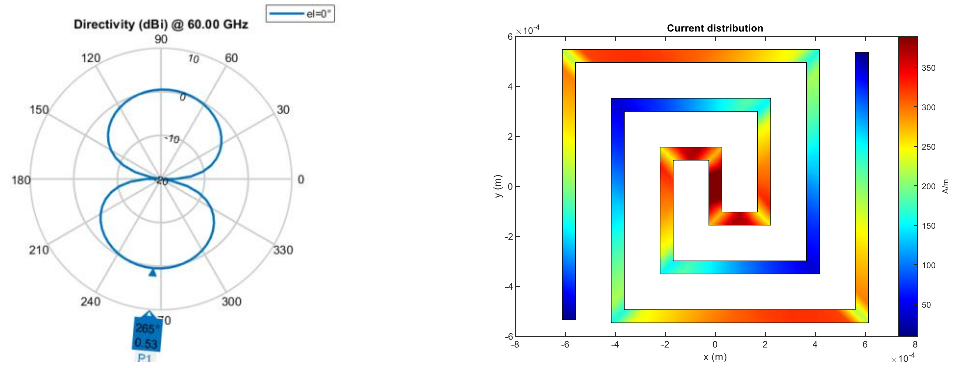

Fig. 4. Behavior at 60 GHz of (a) Directivity Pattern, (b) Current Distribution

The resonance phenomenon at 60 GHz takes center stage in our analysis, accentuated through the insightful depiction of the reflection coefficient S11 (dB) evolution in Fig.3- (b). Here, a conspicuous peak in the reflection coefficient underlines the antenna's resonance at this specific frequency. Fig.4-(a) extends this exploration by spotlighting the antenna's directivity, illustrating its peak performance precisely at 60 GHz.

Fig.4-(b) delves into the intricacies of the antenna's current distribution after 100 iterations, offering a granular understanding of the electric field distribution. This visualization goes beyond a surface-level examination, providing a detailed insight into how electric fields are distributed both along the transverse and normal directions relative to the excitation source. The comprehensive depiction of the current distribution enhances our comprehension of the antenna's behavior, shedding light on the spatial orientation and intensity of electric fields at this critical stage of iteration.

In essence, the combined analysis of Figures Fig.3 and Fig.4 not only reaffirms the resonance characteristics at 60 GHz but also delves deeper into the antenna's performance metrics. The distinct peak in the reflection coefficient, optimal directivity, and nuanced current distribution collectively contribute to a holistic understanding of the antenna's behavior, crucial for informed design decisions and applications.

In summation, the obtained simulation results affirm the stability and efficacy of the numerical approach based on the wave concept. The convergence within a limited number of iterations, resonance behavior, and the consistent agreement with electromagnetic theory collectively validate the reliability and efficiency of the Transverse Wave Approach in addressing the complexities of the printed rectangular spiral antenna.

5. Conclusions

This paper has successfully developed and presented the theoretical groundwork and mathematical underpinnings of the wave concept in the context of numerical electromagnetic methods. The integration of this concept into the transverse wave approach has demonstrated its effectiveness and prowess in electromagnetic investigation and the comprehensive analysis of planar microwave structures across various disciplines.

The diverse simulation results obtained from the examination of a chosen printed rectangular spiral antenna consistently align with electromagnetic theory. These results robustly affirm the validity, stability, and efficiency of the numerical approach anchored in the wave concept. This validation not only contributes significantly to the current understanding but also sets the stage for future developments. It provides a gateway to exploring new trends, including the regeneration or formulation of innovative numerical electromagnetic approaches rooted in the wave concept. These advancements hold the potential to address numerous electromagnetic challenges that traditionally require substantial computational efforts. Moving forward, one promising avenue for future work involves exploring the incorporation of the concept of fictitious magnetic charges into the numerical electromagnetic methods. By considering the theoretical framework of magnetic charges, it may be possible to extend the analysis to a wider range of applications in electrodynamics. This contribution not only advances the existing body of knowledge but also lays the foundation for pioneering methodologies in the dynamic field of electromagnetic research.

Acknowledgements

The authors extend their appreciation to the Deanship of Scientific Research at Northern Border University, Arar, KSA for funding this research work through the project number “NBU-FFR-2024-2942-01".

We also thank the reviewers for their constructive comments, which greatly improved the manuscript.

REFERENCES

[1]. *Meunier, Gérard*, ed. "The finite element method for electromagnetic modeling." (2010).

[2]. *Morgan, Michael A.,* ed. Finite element and finite difference methods in electromagnetic scattering. Elsevier, 2013.

[3]. *Yashiro, K., and S. Ohkawa.* "Boundary element method for electromagnetic scattering from cylinders." IEEE Transactions on Antennas and Propagation 33.4 (1985): 383-389.

[4]. *Temimi, Helmi, Slimane Adjerid, and Mohamed Ayari.* "Implementation of the discontinuous Galerkin method on a multi-story seismically excited building model." Engineering Letters 18.1 (2010): 18.

[5]. *Temimi, Helmi,* A Discontinuous Galerkin Method for Higher-Order Differential Equations Applied to the Wave Equation. Diss. Virginia Tech, 2008.

[6]. *Temimi, Helmi.* "Error analysis of a novel discontinuous Galerkin method for the two-dimensional Poisson's equation." Applied Numerical Mathematics 189 (2023): 130-150.

[7]. *Ayari, Mohamed, Yamen El Touati, and Saleh Altowaijri.* "Method of moments versus advanced transverse wave approach for EM validation of complex microwave and RF applications." Journal of Electromagnetic Engineering and Science 20.1 (2020): 31-38.

[8]. *Yarymbash, Dmytro, et al.* "A new simulation approach of the electromagnetic fields in electrical machines." 2017 International Conference on Information and Digital Technologies (IDT). IEEE, 2017.

[9]. *Almăjanu Florin, et al.* "Radio coverage analysis for mobile communication networks using ics telecom." UPB Sci. Bull., Series C 78.2 (2016): 177-190.

[10]. *DEEP, Ramez EIZDASHIRE ALI, and Radwan KASTANTIN. "*Adaptive design of Costas radar signal with improved narrowband ambiguity function." UPB Sci. Bull. C 82.2 (2020): 127-142.

[11]. *Coman, Cosmin, Ana Barar, and Doina Manaila-Maximean. "*Controlling Electromagnetic Fields in The Terahertz Window with Metal-Dielectric Frequency-Selective Ring Resonators." University POLITEHNICA of Bucharest Scientific Bulletin-Series A-Applied Mathematics and Physics 84.3 (2022): 201-208.

[12]. *Cheng, Raymond, Javad Mashreghi, and William T. Ross*. Function Theory and ℓp Spaces. Vol. 75. American Mathematical Soc., 2020.

[13]. *Huray, Paul G.,* Maxwell's equations. John Wiley & Sons, 2009.

[14]. *Harrington, James A.* "A review of IR transmitting, hollow waveguides." Fiber and Integrated Optics 19.3 (2000): 211-227.

[15]. *Ayari, Mohamed, et al.* "An extended version of Transverse Wave Approach (TWA) for full-wave investigation of planar structures." Journal of Microwaves and Optoelectronics 7.2 (2008): 123-138.
[16]. *Ayari, Mohamed.* "On the Efficiency of the Advanced TWA Approach to the 60-GHz Microstrip Antenna Analysis for 5G Wireless Communication Systems." Engineering, Technology & Applied Science Research 13.1 (2023): 10151-10157.
[17]. *Ayari, Mohamed, Taoufik Aguili, and Henri Baudrand*. "New version of TWA using two-dimensional non-uniform fast Fourier mode transform (2D-NUFFMT) for full-wave investigation of microwave integrated circuits." *Progress In Electromagnetics Research B* 15 (2009): 375-400.
[18]. *Ayari, M., & Altowaijri, S.* (2024). The Efficiency of Surface Impedance Technique in the Transverse Wave Approach for the EM-Modeling of Fractal-Like Tree Structure used in 5G Applications. *Engineering, Technology & Applied Science Research*, *14*(2), 13216-13221.
[19]. *Ayari, M., Aguili, T., & Baudrand, H.* (2009). More efficiency of Transverse Wave Approach (TWA) by applying Anisotropic Mesh Technique (AMT) for full-wave analysis of microwave planar structures. *Progress In Electromagnetics Research B*, *14*, 383-405.
[20]. *Ayari, M., Touati, Y. E., & Altowaijri, S.* (2022). Advanced Transverse Wave Approach for MM-Wave Analysis of Planar Antennas applied in 5G-Technology. *International Journal of Computer Science and Network Security*, *22*(1), 295-299.
[21]. *Malik, Nabeel Ahmed, et al.* "Implantable antennas for bio-medical applications." IEEE Journal of Electromagnetics, RF and Microwaves in Medicine and Biology 5.1 (2020): 84-96.
[22]. *Steinberg, B. Z., & Engheta, N.* (2023). Rest-frame quasistatic theory for rotating electromagnetic systems and circuits. *Physical Review B*, *107*(19).
[23]. *Li, X., Han, B., Zhang, K., Liu, Z., Wang, S., Yan, Y., & Lu, J.* (2024). All-optical dual-axis zero-field atomic magnetometer using light-shift modulation. *Physical Review Applied*, *21*(1), 014023.
[24]. *Wautischer, G., Selyshchev, P., & Schrefl, T.* (2018). Solving the inverse magnetostatic problem using fictitious magnetic charges. *AIP Advances*.
[25]. *Yan, H.* (2010). Three-dimensional magnetic trap lattice on an atom chip with an optically induced fictitious magnetic field. *Physical Review A*, *81*(5), 055401.

APPENDICES

Appendix A

If a unitarity vector space of countable infinite dimension is complete, it is called a Hilbert space. Operators of the Hilbert space define mappings of Hilbert space vectors.

Dirac introduced a compact notation of states and operators by interpreting the expression $\langle\psi|\varphi\rangle$as the inner product of the vectors $\langle\psi|$and$|\varphi\rangle$. Since formally the bracket expression has been subdivided, Dirac has divided the word "braket" also in two parts and introduced the denomination bra-vector for the expression $\langle\psi|$ and ket-vector for the vector $|\varphi\rangle$. In another word, $\langle\psi|$represents matrix of type$(1 \times N)$i.e., row vector and $|\varphi\rangle$ matrix of type$(1 \times N)$i.e., column vector as shown in figure A.1.

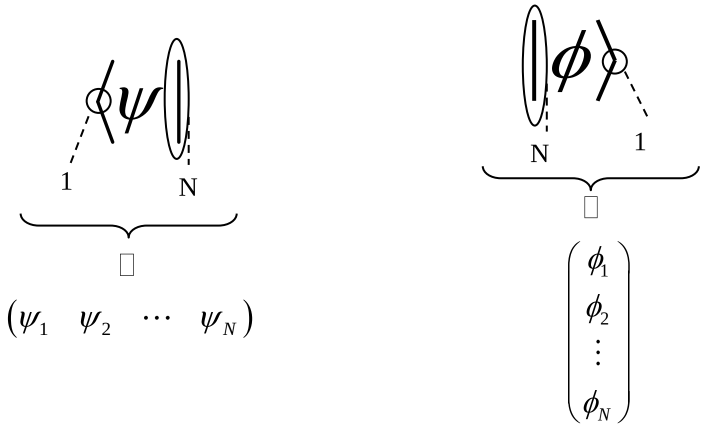

(a) Bra-vector (b) Ket-vector

Fig. 5- Representation of bra and ket-vectors

To any vectors of a Hilbert space is assigned a complex number as a scalar product. In a vector space with a positive definite metric (which we are assuming in the following), a scalar of a vector with itself is positive and real unless the vector is a null vector. The sum of two vectors $|\psi\rangle$ and $|\varphi\rangle$ of Hilbert space again is a vector of Hilbert space.

For this vector we can use the notation $|\psi + \varphi\rangle$and obtain

$$|\psi\rangle + |\varphi\rangle = |\psi + \varphi\rangle \tag{41}$$

The sum of vectors of Hilbert space is commutative and associative.

Appendix B

1. Table 2 meticulously presents Maxwell's equations in integral and differential forms, encompassing various aspects of electromagnetic theory. These equations are fundamental principles governing the behavior of electric and magnetic fields in both spatial and temporal domains. Notably, the table includes formulations of Maxwell's equations that incorporate theoretical considerations of magnetic charges, serving as hypothetical entities representing sources or sinks of magnetic fields. While our research acknowledges the presence of these theoretical constructs within electromagnetic theory, it is essential to clarify that our specific investigation does not directly involve the use or reliance on magnetic charges.

Table2.

Time and phasor domain forms of Maxwell's equations in both integral and differential forms

		Integral Form	Differential Form
Maxwell's Time-domain Equations	Faraday's Law	$\oint_L \mathcal{E}\cdot dl = -\iint_S \left(\frac{\partial \mathcal{B}}{\partial t} + \mathcal{M}\right)\cdot ds$	$\nabla\times\mathcal{E} = -\frac{\partial \mathcal{B}}{\partial t} - \mathcal{M}$
	Ampere's Law	$\oint_L \mathcal{H}\cdot dl = \iint_S \left(\mathcal{J} + \frac{\partial \mathcal{D}}{\partial t}\right)\cdot ds$	$\nabla\times\mathcal{H} = \mathcal{J} + \frac{\partial \mathcal{D}}{\partial t}$
	Electric Gauss' Law	$\oint\!\!\oint_S \mathcal{D}\cdot ds = Q_e$	$\nabla\cdot\mathcal{D} = \rho_v$
	Magnetic Gauss' Law	$\oint\!\!\oint_S \mathcal{B}\cdot ds = Q_m$	$\nabla\cdot\mathcal{B} = \rho_m$
Maxwell's Phasor Domain Equations.	Faraday's Law	$\oint_L E\cdot dl = -\iint_S \left(j\omega B + M\right)\cdot ds$	$\nabla\times E = -j\omega B$
	Ampere's Law	$\oint_L H\cdot dl = \iint_S \left(J + j\omega D\right)\cdot ds$	$\nabla\times H = J + j\omega D$
	Electric Gauss' Law	$\oint\!\!\oint_S D\cdot ds = Q_e$	$\nabla\cdot D = \rho_v$
	Magnetic Gauss' Law	$\oint\!\!\oint_S B\cdot ds = Q_m$	$\nabla\cdot B = \rho_m$

where $\mathcal{E}$ (V/m) is the electric field intensity, $\mathcal{H}$ (A/m) is the magnetic field intensity, $\mathcal{D}$ (C/m2) is the electric flux density, $\mathcal{B}$ (W/m2) is the magnetic flux density, $\mathcal{M}$ (V/m2) is the (fictitious) magnetic current density, $\mathcal{J}$ (A/m2) is the electric current density, Q_e (C/m3) is the electric charge density, and Q_m (C/m3) is the (fictitious) magnetic charge density.

Our primary focus is on analyzing the transmission of electromagnetic waves in specific environments, such as vacuum or hollow waveguides, where the influence of magnetic charges may not be pertinent. Therefore, while the inclusion of magnetic charges in Table 2 provides a comprehensive overview of Maxwell's equations, it is not the central emphasis or premise of our research. Instead, our objective is to investigate the behavior of electromagnetic waves under particular conditions.

2. Table 3 presents the complex propagation constant across several materials. This parameter is essential for defining the propagation of electromagnetic waves through different substances, including both attenuation and phase progression. The table functions as a concise guide for comprehending the variations in wave behavior across various materials, assisting in the development and enhancement of electromagnetic systems.

Table 3

The complex propagation constant for different types of materials

	γ
General form	$\sqrt{j\omega\mu(\sigma + j\omega\varepsilon)}$
Perfect dielectric $(\sigma = 0)$	$j\omega\sqrt{\mu\varepsilon}$
Low-loss dielectric $\left(\frac{\sigma}{\omega\varepsilon} \ll 1\right)$	$\sqrt{\frac{\mu}{\varepsilon}} \cdot \frac{\sigma}{2} + j\omega\sqrt{\mu\varepsilon}$
Good conductor $\left(\frac{\sigma}{\omega\varepsilon} \gg 1\right)$	$\sqrt{\frac{\omega\mu\sigma}{2}} + j\sqrt{\frac{\omega\mu\sigma}{2}}$